THE ASTROPHYSICAL JOURNAL, 452:472–479, 1995 October 10

ELECTRON EXCITATION FUNCTIONS OF THE N_2 SECOND POSITIVE SYSTEM

D. E. SHEMANSKY
Department of Areospace Engineering, University of Southern California Los Angeles, California Los Angeles, CA 90089-1191
AND
J. M. AJELLO AND I. KANIK
Jet Propulsion Laboratory, Pasadena, California 4800 Oak Grove Drive, Pasadena, CA 91109
Received 1995 April 7; accepted 1995 April 24

ABSTRACT

The band strengths of the electron excited N_2 ($C\ ^3\Pi_u$–$B\ ^3\Pi_g$) second positive system (2PG) have been measured in the middle ultraviolet (MUV) range (280–444 nm). The energy dependence of the (0,0) and (1,0) band cross sections is reported with analytic shape functions for use in model calculations. The excitation functions were measured at low pressure to avoid effects of collisional cascade from higher lying states. At low electron energies (11–15 eV), the resolution and energy spacing of the excitation function measurements were sufficient to reveal the importance of threshold effects from resonance processes. The absolute cross section of the 337.14 nm band has a peak value of $1.11 \pm 0.15 \times 10^{-17}$ cm^2 at 14.1 eV. Above 30 eV the cross section decreases with an asymptotic E^{-2} dependence. A spectral analysis of the 2PG band system at 14 and 20 eV has provided relative excited state vibrational level cross sections. The variation of the electronic transition moment over the wavelength range indicated above, has been derived, and an improved transition probability matrix has been obtained. The rate coefficient for solar photoelectron excitation of the (0,0) band is 9.1×10^{-10} cm^3 s^{-1} for photoelectrons above 11.0 eV, a factor of $\sim$1.3 smaller than the previous recommended value.

1. INTRODUCTION

The N_2 [$C\ ^3\Pi_u$–$B\ ^3\Pi_g$ (0,0)] band at 337.14 nm is used as a monitor of the photoelectron flux in the dayglow and secondary electrons in the aurora (Meier 1991; Solomon 1989). The 2PG is chosen for this role since its emission cross section peaks at low energy (10–15 eV). The $C\ ^3\Pi_u$ state is optically forbidden from the $X\ ^1\Sigma_g^+$ state and is not excited by solar fluorescence. The source fluxes of interest have distribution functions which sharply increase in magnitude with decreasing energy. Inversion of N_2 2PG (0,0) band emission intensities to infer photoelectron flux requires accurate electron excitation cross sections in the near threshold region.

The N_2 2PG cross section in the impact energy region between 11 and 15 eV is particularly interesting. There was a rush of activity in the 1970s (Golden, Burns, & Sutcliffe 1974; Kurzweg, Egbert, & Burns 1973; Estler & Doering 1976; Mazeau et al. 1973) to explain the structure in the optical excitation function of the N_2 2PG (0,0) emission as arising from N_2^- resonances that decay to the $C\ ^3\Pi_u$ state by autoionization and collisional cascade from the $E\ ^1\Sigma_g^+$ state. In the resonance process triplet excitation occurs without benefit of an electron exchange but from spontaneous autoionization of the negative ion. Thus the shape of the cross section curve in the threshold energy region, where strong Feshbach and core-excited resonances exist (Schulz 1973), is not a simple fast rise with energy as Cartwright et al. (1977) apparently assumed in linearly extrapolating their data. Other absolute emission experiments performed in the 1960s, 1970s, and 1980s (Jobe, Sharpton, & St. John 1967; Burns, Simpson, & McConkey 1969; Shaw & Campos 1983; Imami & Borst 1974; Shemansky & Broadfoot 1971a, b; Aarts & deHeer 1969) produced cross sections at lower electron energy resolution. There is agreement to 15% in the peak value of the (0,0) band emission cross section as shown in the summary by Shaw & Campos (1983). However, the energy of the peak cross section varies from 14 to 17 eV among the published results. The shape of the cross section in the vicinity of the peak is pressure dependent (Kurzweg et al. 1973, Golden et al. 1974). There is a need to measure the optical excitation function of the 2PG band system at low pressure and, in particular, to tie together the low- and high-energy measurements of cross sections by the many authors cited above.

We present in this paper low pressure optical excitation functions of the 337.03 nm (0,0) band and 315.80 nm (1,0) band at an energy resolution of 0.3 eV with an energy step size of $\sim$0.1 eV. The analysis proceeds as in our recent study of an electron exchange transition involving the excitation of the H_2 ($a\ ^3\Sigma_g^+$) state from the $X\ ^1\Sigma_g^+$ ground state (Ajello & Shemansky 1993). In addition, fully calibrated MUV spectra of the N_2 2PG have been obtained, allowing the tabulation of band cross sections, variation of electronic transition moment, and transition probabilities.

2. EXPERIMENT

The experimental apparatus consists of a medium-resolution 1 m UV spectrometer in tandem with an electron impact collision chamber. The apparatus and experimental technique have been described in detail in previous publications (Ajello et al. 1989, 1992). The UV spectrometer is equipped with a 1200 lines mm^{-1} grating with a dispersion at the exit slit of 0.83 nm mm^{-1}. The detector is an EMR photoelectric trialkali E photomultiplier of exceptionally low dark count of 2 counts s^{-1} at room temperature. The relative sensitivity of the UV spectrometer-detector system was calibrated using a tungsten-halogen blackbody standard lamp of known spectral irradiance. The standard lamp was used to illuminate a calibrated Labsphere Halon diffuser. The diffuser was masked to illuminate the same portion of the grating used in the spectral mea-

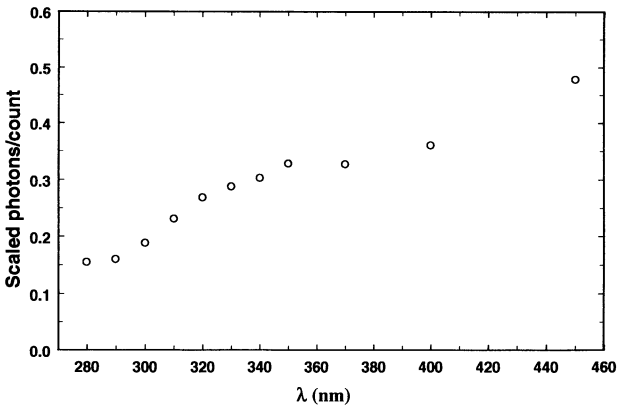

FIG. 1.—The MUV calibration curve for the 1 m spectrometer and photomultiplier detector. The plot shows the relative inverse sensitivity over the range 280–450 nm.

surements with the electron beam. The relative sensitivity of the UV spectrometer-detector system is shown in Figure 1 over the wavelength range 250–450 nm. The accuracy of the relative calibration is 3%. A calibrated spectrum of the 2PG at 14 eV electron energy is shown in Figure 2.

The electron gun was improved to provide an energy resolution of 0.3 eV. The filament design was changed from a hairpin shape to a straight wire. This design reduced the angular divergence of the initial electron trajectories, and allowed operation at a low temperature while extracting enough electron current for a good signal-to-noise ratio. In addition, the diameter of the grid lens element aperture was reduced to 1 mm (Ajello et al. 1988). Smaller apertures reduced path length corrections for a magnetically collimated electron gun, which is particularly important at low electron energy. In addition, care was taken to reduce the number of electron collisions with lens apertures and prevent generation of secondary electrons. The ultimate high-energy experimental capability of a magnetically collimated electron gun for spin-forbidden cross section measurements is found to be 50 eV. Beyond 50 eV, low-energy secondary electrons trapped in the magnetic field measurably affect the excitation function shape. With these design changes the energy resolution in the experiment is determined principally by the tungsten filament operating temperature.

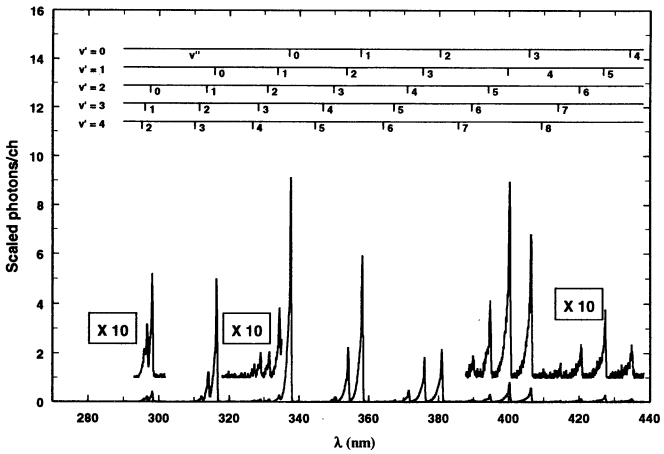

FIG. 2.—The electron impact induced fluorescence MUV spectrum of N_2 at 14 eV, corrected for variation in instrument sensitivity. The spectral resolution is 0.3 nm. The spectrum was obtained in the crossed beam mode at 1×10^{-5} torr background pressure. Band cross sections are given in Table 2.

The absolute cross section for N_2 2PG (0,0) band is determined by comparing the integrated band intensity from N_2^+ (391.4 nm) first negative system (0,0) band to that of the integrated band intensity of N_2 2PG (0,0) band at 40 eV impact energy. For this type of relative flow measurement, in which N_2^+ (391.4 nm) is considered the standard cross section, the instrument is operated in a crossed beam mode. In this mode, a magnetically collimated electron beam intersects a gas beam formed by a capillary array at an angle of 90°. The background gas pressure in the collision chamber is 1×10^{-5} torr. The cross section of N_2^+ 391.4 nm emission at 40 eV is 12.1×10^{-18} cm^2, according to Borst & Zipf (1970). The accuracy of their absolute cross section determination of N_2^+ (391.4 nm) is 10%. The accuracy of the counting statistics in the relative flow calibration at 40 eV is 2%. After a downward 6% correction of the apparent (0,0) band cross section at 40 eV for the estimated secondary electron contribution, the value we obtain is $1.07 \pm 0.15 \times 10^{-18}$ cm^2.

3. EMISSION CROSS SECTIONS

Measurements of the N_2 2PG band excitation functions were obtained with a uniform static gas sample of 1×10^{-5} torr. Emitted photons were detected at 90° to the UV spectrometer. No corrections for polarization of the radiation were made. The emission cross sections and collision strengths for the (0,0) and (1,0) bands, are shown in Figure 3. Figure 4 shows the collision strengths from 10 to 50 eV compared to that of Shemansky & Broadfoot (1971b), Kurzweg et al. (1973), Imami & Borst (1974), Cartwright et al. (1977), and a renormalization of the Cartwright et al. (1977) results by Trajmar et al. (1983). The shape of the cross section was found to be independent of pressure from 1×10^{-6} torr to 1×10^{-4} torr. Other authors have established that above 1×10^{-3} torr, pressure effects arise near the cross section peak from collisional cascade from the metastable E state (Kurzweg et al. 1973; Golden et al. 1974). We find pressure effects in the cross section shape function begin at 1×10^{-4} torr.

A comparison of absolute cross sections from the current work, Trajmar, Register, & Chutjian (1983), Imami & Borst (1974), and Shemansky & Broadfoot (1971a, b), is given in Table 1 for the (0,0) band. A subset of the data points in Figure 4 from this experiment is listed. In Figure 4 or in Table 1, it is clear that the four sets agree to better than 20% at energies above 15 eV. However, in Figure 4, where the threshold region is expanded, the estimated values of Cartwright et al. (1977) are higher by as much as a factor of 3 than the current and Shemansky & Broadfoot (1971a, b) results. The Cartwright et al. (1977) linear interpolation from the peak cross section at 14 eV to threshold overestimates the cross sections, while the Imami & Borst (1974) cross sections fall below the current measurements. The Shemansky & Broadfoot (1971a, b) measurements agree well with the current results after adjustment of the energy scale (Table 1, Fig. 4). It is clear that the FWHM of the cross section peak, found in this experiment, is narrower than the 6 eV FWHM measured by Imami & Borst (1974). We obtain a FWHM of 4.37 eV. Kurzweg et al. (1973) find a FWHM of 4.3 eV. Golden et al. (1974) have shown that a narrower FWHM is obtained at higher gas pressures with 0.3

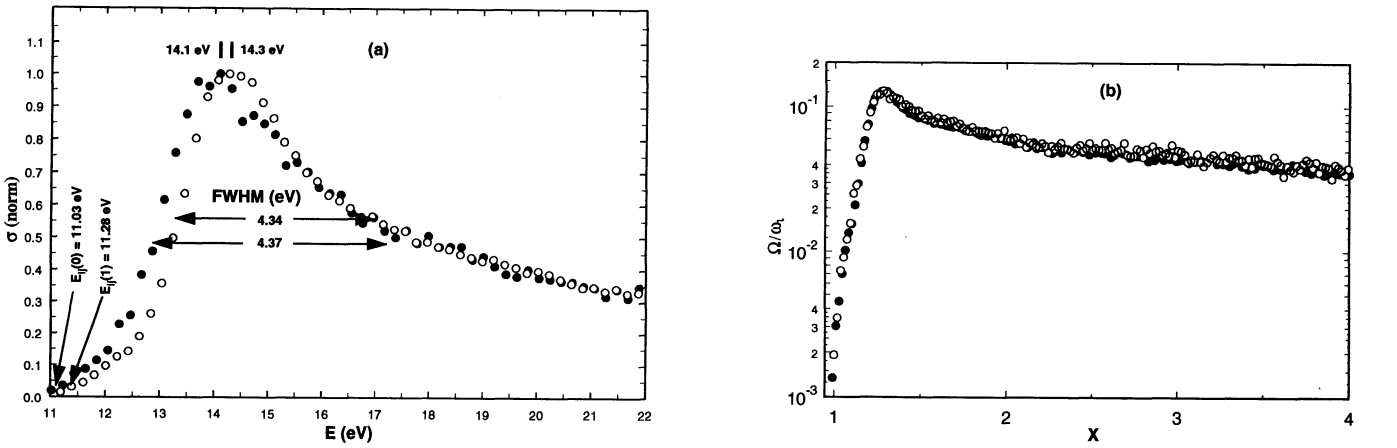

FIG. 3.—(*a*) The relative normalized cross sections of N_2 2PG (0,0) (*solid circles*) and (1,0) (*open circles*) bands. Data points are spaced every 0.1 eV. The cross section measurements were obtained in the static gas mode at 1×10^{-5} torr. (*b*) Collision strengths of the (0,0) (*solid circles*) and (1,0) (*open circles*) bands on a dimensionless energy scale. The (1,0) band is normalized to (0,0).

eV electron resolution when collisional cascade from the E state is induced by experimental conditions.

The threshold structure shown in Figure 4, obtained at low pressure, can be explained without consideration of secondary collisions. Mazeau et al. (1973) report core excited shape and Feshbach resonances at 11.9, 12.14, 12.7, 12.54, 12.78, 12.98, 13.21, 13.45, 13.73, and 13.86 eV that are observed in the differential excitation function measurement of the $E\ ^1\Sigma_g^+$, $v' = 0$, 1 and 2 vibrational levels. Many of these features are sharp with FWHM of 20–100 meV, corresponding to autoionization lifetimes of 10^{-12} to 10^{-13} s. This long lifetime leads to a vibrational sequence which follows the vibrational structure of the E-state and allows coupling to the C state (other exit channels are the E state, and the a'' state). The threshold structure in Figure 4 is indicative of the decay to the C state, $v' = 0$ vibrational level. The E-state cannot promptly radiate to the C-state on the basis of the two electron jump selection rule. Long-lived radiative cascade from the E state is another possible source for populating the C state, although this mechanism does not affect the measurements here. The radiative lifetime of the E-state is ~ 270 μs (Freund 1969). The excited E-state atoms would diffuse far from the field of view of this experiment before radiating. There are no reported measurements of this IR transition at 7786 cm^{-1} (1284 nm).

Kurzweg et al. (1973) used a delay coincidence technique to separate and quantify the (0,0) band emission into a component due to direct excitation and to a component arising from cascade or resonant excitation from the E-state. The delayed emission function revealed many peaks at 12, 12.2, 12.7, and 22 eV. The lifetime of the delayed component had a pressure-dependent lifetime near 10 μs at 20 m Torr. The cascade contribution is small—a maximum of 3% at 22 eV. The most intense remaining C state structure at threshold can be attributed to decay of the negative ion states directly to the C state. This occurs in a time that is fast compared to the 37.4 ns lifetime of the C state (Kurzweg et al. 1973).

The 315.94 nm (1,0) band optical excitation function closely matches the shape of the (0,0) band. The (1,0) and (0,0) band collision strengths are compared in Figure 3*b* on a dimensionless energy (X) scale, with the (1,0) band normalized to the

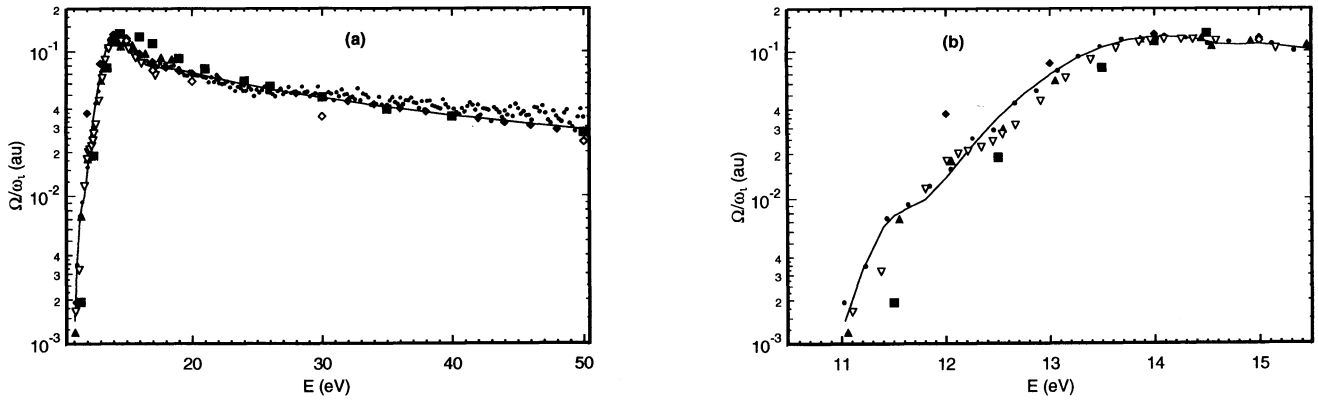

FIG. 4.—Comparison of collision strengths of the N_2 2PG (0,0) band. Model: *solid line*, this work. Data: *solid dots*, this work; *solid squares*, Imami & Borst (1974); *solid triangle*, Shemansky & Broadfoot (1971b); *inverted open triangle*, Kurzweg et al. (1973); *filled diamond*, Cartwright et al. (1977); *open diamond*, Trajmar et al. (1983). (*a*) 10–50 eV. (*b*) Threshold region 10–16 eV.

TABLE 1

N_2 2PG (0,0) AND (1,0) BAND CROSS SECTIONS[a]

(0,0) BAND									(1,0) BAND		
E (eV)	This Work: Data	This Work Model	E (eV)	Imami & Borst 1974	E (eV)	Shemansky & Broadfoot 1971[b]	E (eV)	Trajmar et al. 1983[c]	E (eV)	This Work: Data	This Work: Model
11.23	0.383	0.414	11.03	0.00	11.06	0.129	...		11.40	0.186	0.152
11.64	0.971	0.895	11.5	0.20	11.55	0.759	...		11.60	0.269	0.322
12.05	1.62	1.55	12.5	1.80	12.05	1.78	...		12.01	0.59	0.504
12.46	2.89	3.20	13.5	6.80	12.55	2.81	...		12.42	0.87	0.98
12.67	4.31	4.37	14	10.00	13.05	5.75	...		12.63	1.15	1.41
13.08	6.91	7.03	14.5	11.00	14.55	8.91	...		12.83	1.60	1.93
13.49	9.85	9.56	16	9.50	13.87	10.47	...		13.04	2.19	2.56
14.10	11.26	11.1	17	8.00	14.45	10.2	...		13.45	3.89	3.96
14.72	9.86	8.94	19	5.60	14.92	9.44	...		14.07	6.00	5.62
15.13	9.17	8.97	21	4.30	15.45	8.61	15	9.4	14.48	6.09	5.77
15.54	8.23	7.90	24	3.10	16.45	7.08	...		15.09	5.30	4.77
16.15	7.16	6.46	26	2.62	17.65	6.17	...		15.51	4.61	4.70
17.18	5.87	5.55	30	1.91	18.45	5.75	17	5.1	16.12	3.86	3.85
18.20	5.45	5.11	35	1.35			...		17.15	3.32	3.04
19.02	4.82	4.75	40	1.05			...		18.18	2.89	2.79
20.05	4.24	4.31	50	0.65			20	3.7	19.20	2.65	2.56
25.17	2.56	2.74	60	0.43			...		20.03	2.44	2.37
30.09	2.01	1.92	70	0.30			30	1.4	24.96	1.47	1.54
35.01	1.50	1.42	80	0.22			...		30.10	1.12	1.06
40.14	1.14	1.07	90	0.17			...		35.03	0.839	0.776
100	...	0.174	100	0.13			50	0.56	40.17	0.649	0.59
150	...	0.077	150	0.050							
200	...	0.043	200	0.030							
300	...	0.019	300	0.014							

[a] 10^{-18} cm^2.
[b] Energy scale shifted −0.5 eV.
[c] Total cross section scaled by branching ratio, 0.251.

value of the (0,0) band. The similarity of the band shape functions at different upper vibrational levels has also been noted by Jobe et al. (1967). The location in electron energy (E) and half-width of the (1,0) band is shown in Figure 3*a*. The peak cross section occurs at 14.1 eV, and the FWHM is 4.34 eV. The overplot of the (1,0) and (0,0) bands in Figure 3*a* shows that the threshold effect due to the different onsets of 11.03 and 11.28 eV vanishes near 18 eV. The threshold effect tends to enhance the intensity of $v' = 0$ relative to higher levels. We show this effect in the next section, where the 14 and 20 eV excitation rates of the 2PG are compared.

4. THE N_2 2PG SPECTRUM

The calibrated MUV spectrum of the 2PG obtained at 14 eV is shown in Figure 2. A spectrum at 20 eV has also been obtained, and data are compared in Table 2. The spectrum at 14 eV consists of 2PG features only. The spectrum at 20 eV (not shown) contains some contributions from the first negative band system of N_2^+, fully accounted for in the data reduction. We have analyzed the two spectra for the purpose of determining the total emission cross section for the $C\ ^3\Pi_u$ state and the variation of the electronic transition moment.

The analyses of the two spectra for 14 and 20 eV are shown in Table 2. Values of measured cross sections and normalized rates are compared in Tables 2 and 3. The band identifications are from Pearce & Gaydon (1976), while the band lifetimes and Franck-Condon factors are from Loftus & Krupenie (1977). We have used the upper state transition probabilities to predict emission intensities (Table 2). Table 2 gives the emission cross sections (σ) and relative emission rates ($I_{v'v''}$) for each band based on the equations,

$$I_{v'v''} = g_{v'}\beta_{v'v''}\,, \tag{1a}$$

$$\beta_{v'v''} = \frac{A_{v'v''}}{A_{v'}}\,, \tag{1b}$$

$$g_{v'} = \sigma_{v'}F_e N_{v'''}\,, \tag{1c}$$

where $g_{v'}$ is the excitation rate from the ground state determined by the Franck-Condon factors, $q_{v'0}$, from the $v''' = 0$ level, $\beta_{v'v''}$ is the emission branching ratio, $A_{v'v''}$, $A_{v'}$ are the band and total transition probabilities, and F_e and $N_{v'''}$ are electron flux and ground state population. The calculated and experimental values for $\beta_{v'v''}$ are given in Table 2, along with the cross sections for each band (v', v'') at 14 and 20 eV. Table 3 gives the upper vibrational level excitation rates measured at 14 and 20 eV, compared to the theoretical Franck-Condon factors. Threshold effects are evident with the 14 eV data showing greater strength in the $v' = 0$ level. The (0,0) band is the strongest band in the 2PG system with a measured $I_{00}/I = 0.251$ at 20 eV. The total cross section at 14 eV (the peak cross section) and the total cross section at 20 eV are 4.16×10^{-17} cm^2 and 1.74×10^{-17} cm^2, respectively. The cross section value at 20 eV can be compared to the revised Cartwright et al. (1977) value in Trajmar et al. (1983) of 1.46×10^{-17} cm^2. The results differ by 20%. The cross section value given by Trajmar et al. (1983) at 15 eV is 3.75×10^{-17} cm^2, in much better agreement with the value 3.6×10^{-17} cm^2 obtained here, indicating differences in cross section shape, as shown in Figure 4. This comparison can be considered excellent as Figure 4 indicates for the (0,0) band.

TABLE 2

N_2 2PG Cross Sections (cm^2) and Relative Emission Rates

v′ \ v″	0	1	2	3	4	5	6	7	8	9	$\sigma_{v'}$ [e], $\beta_{v'}$ [c]
0	4.30E-18[a]	3.09E-18	1.23E-19	3.52E-19	9.82E-20	...	...	...	...	...	9.07E-18
	1.11E-17[b]	7.83E-18	3.17E-18	9.58E-19	2.27E-19	...	...	...	...	...	2.33E-17
	0.475[c]	0.338	0.136	0.040	0.010	...	...	...	...	...	1.000
	0.486[d]	0.331	0.130	0.040	0.010	0.002	...	...	...	...	1.000
1	2.43E-18	1.61E-19[f]	1.33E-18	1.14E-19	5.38E-19	1.98E-19	...	...	...	...	5.80E-18
	5.50E-18	3.54E-19[f]	2.95E-18	2.60E-18	1.23E-18	4.35E-19	...	...	...	...	1.32E-17
	0.418	0.027	0.226	0.197	0.093	0.034	...	...	...	...	1.000
	0.434	0.022	0.216	0.190	0.091	0.033	0.010	0.003	...	...	1.000
2	2.16E-19	7.25E-19	6.55E-20	1.38E-19	2.91E-19	2.33E-19	1.17E-19	...	...	...	1.57E-18
	4.09E-19	1.40E-18	1.27E-19	2.71E-19	5.92E-19	4.47E-19	2.13E-19	...	...	...	3.53E-18
	0.127	0.430	0.039	0.082	0.177	0.137	0.067	...	...	...	1.000
	0.135	0.434	0.037	0.083	0.192	0.146	0.071	0.028	0.009		1.000
3	...	1.74E-19[f]	1.42E-19	6.65E-20	...	6.57E-20	3.53E-19[g]	3.42E-20	...	...	5.63E-19
	...	3.03E-19[f]	2.95E-19	1.10E-19	...	9.01E-20	1.32E-19	6.19E-20	...	...	1.34E-18
	...	0.250	0.226	0.093	...	0.082	0.274	0.050	...	...	1.000
	0.007	0.222	0.236	0.129	0.006	0.112	0.137	0.091	0.043	0.0018	1.000
4	...	...	...	...	2.57E-20	...	...	...	...	...	1.43E-19
	...	...	...	...	4.88E-20	...	...	...	...	...	2.71E-19
	...	...	...	...	0.180	...	...	...	...	...	1.000
	...	0.008	0.283	0.121	0.210	0.007	0.058	0.131	0.115	0.068	1.000

[a] $\sigma_{v'v''}$ (20 eV).
[b] $\sigma_{v'v''}$ (14 eV).
[c] $\beta_{v'v''}$, measured; $\beta_{v'} = \Sigma_{v''} \beta_{v'v''}$.
[d] $\beta_{v'v''}$, model.
[e] Estimated total cross sections, $\sigma_{v'} = \Sigma_{v''} \sigma_{v'v''}$; $\Sigma_{v'} \sigma_{v'}$ (20 eV) = 1.74×10^{-17}; $\Sigma_{v'} \sigma_{v'}$ (14 eV) = 4.16×10^{-17}.
[f] Blended with other N_2 2PG bands.
[g] Blended with N_2^+ 391.4 nm band.

TABLE 3

N_2 $C\ ^3\Pi_u$ STATE RELATIVE EXCITATION RATES

v'	0	1	2	3	4
$q_{v'0}$[a]	0.547	0.305	0.106	0.030	0.008
$g_{v'0}$ (14 eV)[b]	0.560	0.317	0.085	0.032	0.007
$g_{v'0}$ (20 eV)[b]	0.529	0.338	0.092	0.033	0.008

[a] Theoretical Franck-Condon factors.
[b] This work, measured excitation rates.

It is possible to deduce the variation in the electronic transition moment from the relative band intensities. We use the expression,

$$I_{v'v''} = N_{v'} R_e^2(r_{v'v''}) q_{v'v''} / \lambda^3_{v'v''} , \quad (2)$$

for the intensity of a band, $I_{v'v''}$, where $N_{v'}$ is the number density in v', $R_e(r_{v'v''})$ is the electronic transition moment, and $r_{v'v''}$ is the mean internuclear distance in transition (v', v'') of wavelength $\lambda_{v'v''}$. The normalized data for the v' progressions are given in Table 2. The band intensity data for the analysis is taken from the data shown in Figure 2. The variation of the electronic transition moment has been measured by Nicholls (1964), Tyte (1962), Jain & Sahni (1967), and Hartman & Johnson (1978).

The analysis of the present data gives a relationship

$$R_e(r_{v'v''}) \propto \{[(-0.763917 r_{v'v''} + 2.464191) r_{v'v''} - 2.669743] r_{v'v''} + 1\} , \quad (3)$$

Figure 5 shows the normalized data compared to equation (3) and the previous analytic results by Jain & Sahni (1967), Hartman & Johnson (1978), and Tyte (1962). The earlier Tyte (1962) linear function is in satisfactory agreement with the present work, while significant shape differences are indicated with the other two analyses. The present variation in R_e predicts that the lifetime of the upper state varies by a factor of $\sim$35% between the $v' = 0$ and $v' = 3$ levels. Table 4 gives the calculated transition probabilities using (3) and the lifetimes recommended by Loftus & Krupenie (1977).

Significant differences beyond experimental error between calculated and measured relative band strengths appear in the $v' = 3$ and 4 progressions as shown in Table 2. This may be attributed partly to statistical uncertainty in the weak bands and blended features, rather than intrinsic properties of the transition.

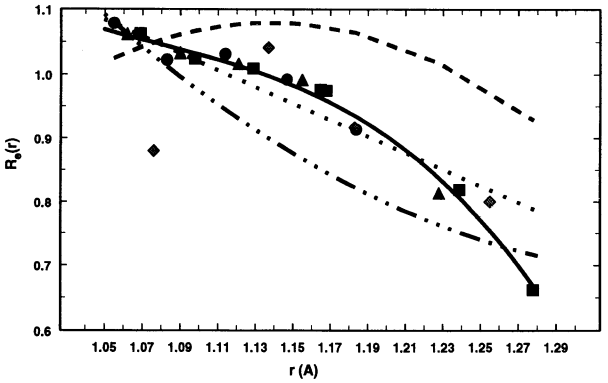

FIG. 5.—Variation of the electronic transition moment of the N_2 2PG system. Model: *solid line*, this work; *dotted line*, Tyte (1962); *dashed line*, Jain & Sahni (1967); *dash dotted line*, Hartman & Johnson (1978). Data: this work, *circles*, $v' = 0$; *triangles*, $v' = 1$; *squares*, $v' = 2$; *diamonds*, $v' = 3$.

5. ANALYTIC EXCITATION FUNCTIONS

The emission cross sections measured in the present experiment have been approximated using analytic expressions that allow accurate determination of excitation rates at any electron energy. The resonance contributions to the cross sections are approximated by error functions that account for the envelope of the resonant structure. It is assumed that electron energy distributions are broader than $\sim$0.3 eV. The N_2 2PG (0,0) band cross section has been approximated by the sum of two error functions in collision strength, and an additional expression that has been utilized in earlier work (cf. Shemansky et al. 1985a, b; Ajello & Shemansky 1993). The collision strengths for the error function components, in both monoenergetic [$\Omega_{ij}(X)$], and thermally averaged [$\Omega_{ij}(T_e)$] forms are given by the expressions

$$\Omega_{ij}(X) = C_0 \exp[-C_1^2(X - C_2)^2] , \quad (4a)$$

$$\Omega_{ij}(T_e) = \frac{C_0}{2C_1}\left[\pi^{1/2} - \Gamma\left(\frac{1}{2}, Z_0^2\right)\right] Y \times \exp\left[-Y\left(C_2 - 1 - \frac{Y}{4C_1^2}\right)\right] , \quad (4b)$$

$$Z_0 = C_1(1 - C_2) + \frac{Y}{2C_1} . \quad (4c)$$

TABLE 4

N_2 2PG TRANSITION PROBABILITIES (10^6 s^{-1})

$v' \backslash v''$	0	1	2	3	4	5	6	7	8	9	$A_{v'}$
	337.029[a]	357.576	380.376	405.807	434.336	466.550	503.194	545.234	593.936		
0	13.542[b]	9.204	3.628	1.108	0.289	0.069	...	...	...	...	27.84
	315.801	333.773	353.555	375.422	399.711	426.833	457.301	491.759	531.033	...	
1	11.553	0.590	5.766	5.074	2.435	0.884	0.271	0.077	...	...	26.65
	297.564	313.467	330.852	349.926	370.936	394.180	420.023	448.915	481.417	...	
2	2.953	9.462	0.796	1.806	4.179	3.187	1.554	0.608	0.206	...	21.80
	2281.847	296.074	311.536	328.391	346.826	367.065	389.374	414.079	441.578	472.300	
3	0.145	4.921	5.241	2.861	0.129	2.492	3.039	2.009	0.964	0.389	22.19
	268.373	281.242	295.157	310.243	326.646	344.537	364.119	385.635	409.377	435.500	
4	...	0.150	5.207	2.224	3.849	0.125	1.067	2.398	2.112	1.240	18.37

[a] Wavelength, $\lambda_{v'v''}$ (nm), band origin.
[b] $A_{v'v''}$.

The quantities C_n are constants, X is the dimensionless electron energy, and Y is the Boltzmann term,

$$X = \frac{E}{E_{ij}}, \tag{5a}$$

$$Y = \frac{E_{ij}}{kT_e}, \tag{5b}$$

where E is electron energy, E_{ij} is the threshold energy for excitation, and T_e is the electron temperature.

The additional function utilized in fitting the total collision strength is given by the equations

$$\Omega_{ij}(X) = C_n X^{-n} + \frac{C_6}{X} \tag{6a}$$

$$\Omega_{ij}(T_e) = [C_n E_n(Y) + C_6 E_1(Y)] Y \exp(Y) \tag{6b}$$

where the $E_n(Y)$ are exponential integrals of order n. In this case the C_6 term determines the high energy asymptotic energy dependence of the cross section. The excitation cross section is given by the equation,

$$\sigma_{ij}(X) = \frac{\Omega_{ij}(X)}{\omega_i E_{ij} X}, \tag{7}$$

where σ_{ij} is the excitation cross section in atomic units, ω_i is lower state degeneracy and E_{ij} is the transition energy in rydberg units.

The rate coefficient (Q_{ij}) for thermal electrons in units of cm^3 s^{-1} is given by

$$Q_{ij}(T_e) = (2.173 \times 10^{-8}) \left(\frac{Y}{E_{ij}}\right)^{1/2} \left[\frac{\Omega_{ij}(T_e)}{\omega_i}\right] \exp(-Y) \tag{8}$$

for E_{ij} in Rydbergs.

The $C\ ^3\Pi_u$–$B\ ^3\Pi_g$ (0,0) and (1,0) band emission cross sections have been fitted using the data shown in Table 1. The analytic fit is the summation of two terms of the form (4) and one term of the form (6). The constants are listed in Table 5. The model and data are compared in Table 1 and Figure 4. Notable aspects of the model are finite cross section values at threshold and an asymptotic E^{-2} dependence at high energy. The predicted high energy values are in reasonable agreement with the results obtained by Imami & Borst (1974), as shown in Table 1. Note that summation of strengths from equations (4) and (6) must be made at common values of electron energy (E), rather than at common values of dimensionless energy (X). Figure 4 shows plots of the collision strength in comparison with the various measurements. Above 28 eV the model calculation tends to fall below the current measured data, attributed to the effect of secondary electrons in the experimental system.

6. DISCUSSION AND CONCLUSIONS

The most critical factor in relating the emission rate of the N_2 ($C\ ^3\Pi_u$–$B\ ^3\Pi_g$) system in the dayglow and aurora to the low-energy electron flux is knowledge of the near threshold cross section. The accumulated results in the laboratory experiments discussed here appear to have established the excitation functions with satisfactory accuracy. In order to make the application of cross sections to rate calculations more convenient, we have utilized a model to establish accurate analytic fits to the data. Equations (4)–(8) are applied with coefficients given for the N_2 2PG (0,0) and (1,0) bands in Table 5. The coefficients can be scaled for other bands in the $v' = 0$ and 1 progressions. The measurements obtained here indicate that the $v' = 2$–4 levels have cross section shapes measurably different from the $v' = 0$ and 1 levels. The analytic functions produce a small finite cross section value at threshold and a variable shape function leading up to the peak at 14.1 eV for the (0,0) band, matching the observations (Fig. 4*a*). The high-energy asymptote is determined by equation (6), which produces an E^{-2} cross section dependence, characteristic of electron exchange excitation.

The more recent publications concerned with dayglow excitation have utilized the less accurate cross section data, that may in some cases produce misleading conclusions. The effective rate coefficients for the excitation of the N_2 1PG (0,0) band by dayglow photoelectrons have been calculated here using the present and earlier cross sections utilized in dayglow research. These values are shown in Table 6. The rate coefficients refer to that part of the photoelectron population above the excitation threshold of the N_2 2PG (0,0) band, given by

$$Q_{ij}(ph_e) = \left[\frac{2(1.6 \times 10^{-12})}{m_e}\right]^{1/2} \frac{\int_{E_{ij}} 4\pi \mathcal{F}_e \sigma_{ij}(E) E^{-1/2}\, dE}{\int_{E_{ij}} 4\pi \mathcal{F}_e E^{-1}\, dE} \tag{9}$$

in units of $cm^3\ s^{-1}$, where $\mathcal{F}_e$ (electrons $cm^{-2}\ sr^{-1}\ eV^{-1}$) is the differential photoelectron flux, and m_e is the mass of the electron.

The Cartwright et al. (1977) cross sections recommended by Meier (1991) produce rates a factor of ~1.4 larger than the values obtained with the present cross section. The rate calculated by Hernandez et al. (1983), using the Imami & Borst (1974) cross section, is 17% below the value obtained here.

Meier (1991) has recommended the use of the Cartwright et al. (1977) excitation cross sections for interpretation of UV photometer N_2 2PG (0,0) band dayglow observations.

TABLE 5

CROSS SECTION COEFFICIENTS

Equation Number	n	C_0	C_1	C_2	C_6	E_{ij} (eV)
A. For N_2 2PG (0,0) Band						
7	18.0	−0.0988193	...	...	0.0988193	14.69
5	...	0.003621	37.08	1.04	...	11.03
5	...	0.1297	7.856742	1.278	...	11.03
B. For N_2 2PG (1,0) Band						
7	18.0	−0.053255	...	...	0.053255	15.02
5	...	0.0019515	37.08	1.04	...	11.28
5	...	0.069928	7.856742	1.278	...	11.28

TABLE 6

N_2 2PG (0,0) BAND SOLAR PHOTOELECTRON RATE COEFFICIENTS

Q^a (10^{-10} cm^3 s^{-1})	Reference
9.11	1
7.79	2
11.73	3
9.92	3[b]

[a] Effective rate coefficient for the solar photoelectron population above 11.0 eV. The photoelectron flux utilized in the calculation is from Hernandez et al. (1983; rate coefficients are indistinguishable for the flux distributions given for 220 and 160 km altitudes.

[b] Cartwright et al. 1977 cross section shape function scaled by Trajmar et al. 1983 correction factor.

REFERENCES.—(1) This work; (2) Imami & Borst 1974; (3) Cartwright et al. 1977.

However, Cartwright et al. (1977) did not measure the $C\ ^3\Pi_u$ state cross section in the threshold region. Trajmar et al. (1983) has verified that this is the case in their review of the revised N_2 cross section of the $C\ ^3\Pi_u$ state, citing measurements at energies of 15, 17, 20, 30, and 50 eV. The Cartwright et al. (1977) estimates below 15 eV are extrapolations and should not be used in aeronomical modeling. Solomon (1989) has utilized the revised Trajmar et al. (1983) values with the shape function of Cartwright et al. (1977), resulting in a rate that is a factor of $\sim$1.1 larger (Table 6) than the value recommended in the present work. The effective rate coefficient for excitation of the N_2 2PG (0,0) band based on the cross section derived here is 9.1×10^{-10} cm^3 s^{-1} using the photoelectron population above 11 eV as reported by Hernandez et al. (1983).

The variation of electronic transition moment has been measured for the N_2 $C\ ^3\Pi_u$–$B\ ^3\Pi_g$ system. The results are in basic agreement with the earlier work by Tyte (1962), but in significantly less satisfactory agreement with Jain & Sahni (1967) and Hartman and Johnson (1978) (Fig. 5). A new polynomic variation with $r_{v'v''}$ has been derived and is given by equation (3), valid over the range 1.05–1.3 Å. The transition probabilities obtained from the new transition moment have been calculated and are given in Table 4.

The authors acknowledge the valuable contributions of R. W. Carlson for assistance with spectrograph calibration, E. Bethke for data reduction support, and R. I. Multari for electron gun model calculations. The research described in this publication was carried out by the Jet Propulsion Laboratory, California Institute of Technology, and the University of Southern California. The work at the University of Southern California was supported by National Science Foundation grant ATM-93 20589. The work at the Jet Propulsion Laboratory was supported by funds from the University of Southern California, the Air Force Office of Scientific Research (AFOSR), and the NASA Planetary, Space Physics and Astronomy Program Offices through an agreement with the National Aeronautics and Space Administration.

REFERENCES

Aarts, J. F. M., & deHeer, F. J. 1969, Chem. Phys. Lett., 4, 116
Ajello, J. M., James, G. K., Franklin, B. O., & Shemansky, D. E. 1989, Phys. Rev. A, 40, 3524
Ajello, J., James, G. K., Kanik, I., & Franklin, B. O. 1992, J. Geophys. Res., 97, 10473
Ajello, J. M., & Shemansky, D. E. 1985, J. Geophys. Res., 90, 9845
———. 1993, ApJ, 407, 820
Ajello, J. M., et al. 1988, Appl. Opt., 27, 890
Borst, W. L., & Zipf, E. C. 1970, Phys. Rev. A, 1, 834
Burns, D. J., Simpson, F. R., & McConkey, J. W. 1969, J. Phys. B, 2, 52
Cartwright, D. C., Trajmar, S., Chutjian, A., & Williams, W. 1977, Phys. Rev. A, 16, 1041
Estler, R. C., & Doering, J. P. 1976, J. Chem. Phys., 65, 1406
Freund, R. S. 1969, J. Chem. Phys., 50, 3734
Golden, D. E., Burns, D. J., & Sutcliffe, V. C. 1974, Phys. Rev. A, 10, 2123
Hartmann, G., & Johnson, P. C. 1978, J. Phys. B, 11, 1597
Hernandez, S. P., Doering, J. P., Abreu, V. J., & Victor, G. A. 1983, Planet. Space Sci., 31, 221
Imami, M., & Borst, W. L. 1974, J. Chem, Phys., 61, 1115
Jain, D. C., & Sahni, R. C. 1967, J. Quant. Spectrosc. Rad. Transf., 7, 475
Jobe, J. D., Sharpton, F. A., & St John, R. M. 1967, J. Opt. Soc. Am., 57, 106
Kurzweg, L., Egbert, G. T., & Burns, D. J. 1973, Phys. Rev. A, 7, 1966
Lofthus, A., & Krupenie, P. H. 1977, J. Chem. Phys., 6, 113
Mazeau, J. R., Hall, R. I., Joyez, G., Landau, M., & Reinhardt, J. 1973, J. Phys. B, 6, 873
Meier, R. R. 1991, Space, Sci. Rev., 58, 1
Nicholls, R. W. 1964, Ann. Geophys., 20, 144
Pearse, R. W. B., & Gaydon, A. G. 1976, in The Identification of Molecular Spectra (New York: Wiley)
Schulz, G. J. 1973, Rev. Mod. Phys., 45, 423
Shaw, M., & Campos, J. 1983, J. Quant. Spectrosc. Rad. Transf., 30, 73
Shemansky, D. E., Ajello, J. M., & Hall, D. T. 1985a, ApJ, 296, 765
Shemansky, D. E., Ajello, J. M., Hall, D. T., & Franklin, B. 1985b, ApJ, 296, 774
Shemansky, D. E., & Broadfoot, A. L. 1971a, J. Quant. Spectrosc. Rad. Transf., 11, 1385
———. 1971b, J. Quant. Spectrosc. Rad. Transf., 11, 1401
Solomon, S. C. 1989, J. Geophys. Res., 94, 17215
Trajmar, S., Register, D. F., & Chutjian, A. 1983, Phys. Rep., 97, 219
Tyte, D. C. 1962, Proc. Phys. Soc., 80, 1347